Marine Biology (2018) 165:104
https://doi.org/10.1007/s00227-018-3362-7

ORIGINAL PAPER

Assimilation, translocation, and utilization of carbon between photosynthetic symbiotic dinoflagellates and their planktic foraminifera host

Charlotte LeKieffre[1,2] · Howard J. Spero[3] · Ann D. Russell[3] · Jennifer S. Fehrenbacher[3,4] · Emmanuelle Geslin[2] · Anders Meibom[1,5]

Received: 1 December 2017 / Accepted: 7 May 2018 / Published online: 19 May 2018

Abstract

Some species of planktic foraminifera inhabiting oligotrophic surface water environments are in an obligate symbiotic relationship with dinoflagellate microalgae, which can assimilate carbon (C) through photosynthesis. However, the mechanism and dynamics of C photosynthate translocation to the foraminiferal host, and related benefits for the dinoflagellates in this symbiotic association, are poorly constrained. As a consequence, the role of planktic foraminifera as autotroph organisms in ocean surface ecosystems is not well understood. Here, we performed pulse-chase experiments with ^{13}C-enriched dissolved inorganic carbon, followed by TEM and quantitative NanoSIMS isotopic imaging to visualize photosynthetic C assimilation by individual symbiotic dinoflagellates and subsequent translocation to their *Orbulina universa* host. Although most of the dinoflagellate population migrates out of the host endoplasm onto external spines during the day, our observations show that a small fraction remains inside the host cell during daytime. All symbionts, whether outside or inside the foraminifera cell, effectively assimilate C into starch nodules during daytime photosynthesis. At the onset of night, all dinoflagellates from the exterior spine–ectoplasm region migrate back into the foraminiferal cell. During the night, respiration by dinoflagellates and carbon translocation to the host, likely in the form of lipids, greatly reduces the abundance of starch in dinoflagellates. Dinoflagellate mitosis is only observed at night, with a substantial contribution of carbon fixed during the previous day contributing to the production of new biomass.

Responsible Editor: K. Bischof.

Reviewed by L. Polerecky and undisclosed experts.

Electronic supplementary material The online version of this article (https://doi.org/10.1007/s00227-018-3362-7) contains supplementary material, which is available to authorized users.

✉ Charlotte LeKieffre
charlotte.lekieffre@epfl.ch

1 Laboratory for Biological Geochemistry, School of Architecture, Civil and Environmental Engineering (ENAC), Ecole Polytechnique Fédérale de Lausanne (EPFL), Lausanne, Switzerland

2 UMR CNRS 6112-LPG-BIAF, Université d'Angers, 49045 Angers Cedex, France

3 Department of Earth and Planetary Sciences, University of California Davis, Davis, CA 95616, USA

4 College of Earth, Ocean, and Atmospheric Sciences, Oregon State University, Corvallis, OR 97331, USA

5 Center for Advanced Surface Analysis, Institute of Earth Sciences, University of Lausanne, Lausanne, Switzerland

Introduction

The intracellular association between photosynthetic dinoflagellate algae and foraminifera has been recorded in numerous studies of large benthic (Lee 1983; Leutenegger 1984) and planktic foraminifera species (Rhumbler 1911; Lee et al. 1965; Anderson and Bé 1976; Bé et al. 1977; Spero and Parker 1985; Spero 1987), and the symbiotic nature of this relationship confirmed by the observed effects of the dinoflagellates on host metabolism and growth. For example, in large benthic foraminifera, such as *Heterostegina depressa*, *Amphistegina lessonii*, and *Archaias angulatus*, the symbionts were shown to enhance growth rate (Duguay and Taylor 1978; Lee and Zucker 1969; Röttger and Berger 1972). In planktic species, such as *Globigerinoides sacculifer*, dinoflagellate symbiont photosynthesis affects final shell size, and elimination of symbionts results in earlier gametogenesis and reduced lifespan (Bé et al. 1982). Studies with micro-sensors have shown that significant changes in oxygen production and pH in planktic

Orbulina universa were correlated with variations in light level, demonstrating the effect of symbiotic dinoflagellate photosynthesis on the host cell micro-environment (Rink et al. 1998; Köhler-Rink and Kühl 2005). In *G. sacculifer*, longer survival rates have been recorded in unfed specimens exposed to high light levels (= elevated photosynthetic rates) in comparison with unfed specimens kept under low-light conditions (Caron et al. 1981), suggesting that the dinoflagellates are providing photosynthates to the foraminiferal host cell. Although symbiotic Sarcodines such as foraminifera are important contributors to primary production in oligotrophic environments around the world (Spero and Parker 1985; Caron et al. 1995), no studies have documented the timing, extent, and distribution of translocated organic C photosynthates between symbiotic dinoflagellates and their foraminiferal host cells.

Here, we present correlated transmission electron microscopy (TEM) and nanoscale secondary ions mass spectrometry (NanoSIMS) images of the intracellular distribution of assimilated carbon in *O. universa* from ^{13}C-enriched pulse-chase experiments with high temporal resolution (minutes to hours) across a full diurnal cycle. The NanoSIMS ion microprobe permits subcellular, quantitative isotopic imaging of biological tissue and is directly correlated with TEM ultrastructural imaging (Hoppe et al. 2013; Nuñez et al. 2018). Combined with isotopic pulse-chase labeling experiments, this allows metabolic pathways to be studied at the subcellular level in other symbiotic marine organisms, such as corals or phytoplankton (Clode et al. 2007; Pernice et al. 2012, 2015; Ceh et al. 2013; Kopp et al. 2013, 2015a, b; Krupke et al. 2015). Two recent studies also used NanoSIMS to study foraminifera metabolism (Nomaki et al. 2016; LeKieffre et al. 2017). The primary objective of this study was to visualize and quantify carbon uptake, incorporation, and photosynthate translocation between dinoflagellate symbionts and host in the planktic foraminifer *O. universa*.

Materials and methods

Collection of the foraminifera

Specimens of *O. universa* were hand-collected by SCUBA divers from surface waters, 1–2 km north of Santa Catalina Island (California, USA) in August, 2014. The specimens were individually collected in glass jars from a depth of 2–6 m in the San Pedro Basin and transported within 1 h to the laboratory at the University of Southern California Wrigley Marine Science Center. Each individual was then transferred with a glass pipette to a clean glass jar containing 0.45 µm filtered seawater and maintained at 22 °C. Light micrographs were taken of living specimens, both in light and after acclimation to the dark, using a Nikon D3200 digital SLR camera connected to a Nikon TMS inverted microscope.

Experiment: incubation with $NaH^{13}CO_3$ in light

Approximately 1 day after collection, 24 pre-sphere (trochospiral test) *O. universa* were selected and fed a 1-day-old *Artemia salina* brine shrimp nauplius 4 h prior to the ^{13}C-incubation experiment. At 13:00 local time (i.e., corresponding to maximum symbiont photosynthetic rate (P_{max})) (Spero and Parker 1985), 21 fed specimens were transferred into 22 mL scintillation vials (one specimen per vial), filled with 0.45 µm filtered seawater spiked by the addition of 2 mM $NaH^{13}CO_3$ (^{13}C fraction of 99%, Cambridge Isotopes Laboratory Inc.) (pH 8.2, measured after the addition of $NaH^{13}CO_3$). The addition of the spike resulted in a final dissolved inorganic carbon (DIC) concentration of ~ 4 mM and a DIC $^{13}C/^{12}C$ ratio ~ 0.45. The capped vials were then immersed into water baths held at 22 °C under artificial light (Sylvania F24T12 'Cool White' fluorescent lights). The lights have a minimum intensity of 350 µmol photons m^{-2} s^{-1}, which is the P_{max} light saturation threshold for symbiont photosynthesis in this species (Spero and Parker 1985; Rink et al. 1998). Three individuals were maintained in unspiked filtered seawater under identical conditions to serve as control specimens. After 6 h (Fig. 1), the isotopic incubation was terminated and a chase phase began by transferring foraminifera to new vials filled with ambient 0.45 µm filtrated seawater (i.e., natural DIC $^{13}C/^{12}C \approx 0.01$) with a DIC concentration of ca. 2 mM. Specimens were transferred through an intermediate wash vial to avoid increasing the $\delta^{13}C_{DIC}$ of the ambient chase solution. The vials were placed in the dark for 12 h and then moved back into the light for an additional 12 h period. During this 30 h experiment, three specimens were sampled for TEM fixation at the following timepoints: 0, 0.75, 2, 6, 7, 12, 18, and 30 h, respectively, as indicated in Fig. 1.

A second incubation experiment was carried out using the same protocol described for the main experiment, except

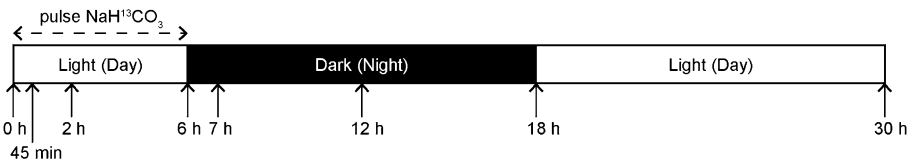

Fig. 1 *O. universa* incubation experiment time line. Three specimens were sampled at each timepoint indicated with arrows. Details in the text

that the three specimens were incubated in ^{13}C spike for 6 h in the dark. The pulse phase of this experiment was initiated at 13:00 local time and the specimens were kept in darkness for 6 h. They were then collected for TEM fixation and processed as the other samples, described below.

TEM–NanoSIMS sample preparation

At each sampling timepoint, the collected *O. universa* specimens were individually transferred into 0.5 mL micro-centrifuge tubes containing filtered seawater with 4% glutaraldehyde and 2% paraformaldehyde (pH 8.1), and fixed for 24 h at room temperature. The fixative solution was then replaced by a solution of 2% glutaraldehyde in filtrated seawater for transport to the Electron Microscopy Facility, University of Lausanne, Switzerland. During transport, the majority of spines were broken and most of the reticulopods and symbiotic microalgae attached to the spines were lost, but ectoplasmic matrix adjacent to the outside of the test was well preserved (see below). Upon arrival, specimens were rinsed in artificial seawater (RedSea Salt, 34 psu), then post-fixed with a solution of 2% OsO_4 diluted in distilled water for 1 h. After thorough rinsing with distilled water, all specimens were embedded in 3% Agar (Sigma-Aldrich, type VII-A, low gelling temperature), following the procedure described by Spero (1988). This step protected the fixed foraminifera during the decalcification and dehydration steps, and preserved the natural positioning of the symbiotic dinoflagellates that were present at the base of the broken spines on the outer shell surface. The agar-embedded foraminifera were then decalcified in two successive baths (1 and 48 h, respectively) of EDTA 0.1 M diluted in distilled water, followed by a dehydration series of increasing ethanol concentrations (50, 70, 95, and 100%). Samples were prepared for TEM at room temperature using a sequential LR White resin impregnation first with a solution of resin/ethanol 100% (volume 1:1) for 1 h, followed by pure resin for 8 h. Finally, all specimens were placed in a third bath of pure resin for 3 h and then allowed to cure in solid resin at 70 °C for 8 h. Specimens were sliced with an ultramicrotome (Reichert Ultracut S) equipped with a diamond knife (Diatome Ultra, 45°) into semi-thin (500 nm) and ultra-thin (70 nm) sections. Semi-thin sections were stained with a mix of toluidine blue and basic fuchsine prior to observation under a light microscope. The ultra-thin sections were placed on formvar–carbon-coated copper grids (Electron Microscopy Science, reference FCF200F1-Cu), stained with 2% uranyl acetate for 10 min and observed with a transmission electron microscope (TEM, Philips 301 CM100, 80 kV). Areas of interest for NanoSIMS imaging were selected from TEM images.

NanoSIMS analytical procedures followed those described in Lekieffre et al. (2017). Briefly, following TEM imaging, the same ultra-thin sections were coated with about 10 nm gold prior to imaging with a Cameca NanoSIMS 50L ion microprobe (Hoppe et al. 2013). NanoSIMS images were obtained by bombarding thin sections with a beam of Cs^+ focused to a spot size of ~ 150 nm (beam current ~ 2 pA) and counting $^{12}C^{12}C^-$, $^{13}C^{12}C^-$, and $^{12}C^{14}N^-$ ions in electron multipliers at a mass resolution of > 8000 (Cameca definition), enough to resolve potential interferences in the mass spectrum. NanoSIMS images were drift-corrected and ^{13}C-enrichments quantified by forming the ratio $^{12}C^{13}C^-/^{12}C_2^-$, reported in ‰ deviation from a standard $^{13}C/^{12}C$ ratio:

$$\delta^{13}C(‰) = \left(\frac{C_{meas}}{C_{control}} - 1\right) \times 1000,$$

where C_{meas} is the $^{12}C^{13}C^-/^{12}C_2^-$ ratio measured in the isotopically labeled samples, and $C_{control}$ is the $^{12}C^{13}C^-/^{12}C_2^-$ ratio measured on control samples incubated without ^{13}C-addition (see above), prepared, and handled in an identical manner. Note that the precision of the $^{13}C/^{12}C$ ratios obtained with NanoSIMS imaging does not permit the resolution of natural isotopic variations in the tissue (e.g., diurnal), or variations between organelles. The average $^{13}C/^{12}C$ ratio of the endoplasm of three control specimens was, therefore, used as the standard ratio against which the (very large) experimental ^{13}C-enrichments were quantified (cf. equation above); the reported ^{13}C-enrichments are, therefore, not relative to the VPDB standard. Control values were measured at the beginning and the end of each NanoSIMS session and exhibited no significant analytical drifts.

NanoSIMS image processing was carried out as described in LeKieffre et al. (2017) and Nomaki et al. (2018). Briefly, TEM images were aligned with corresponding NanoSIMS $^{12}C^{14}N^-$ images (Online Resource 1) using the software Look@NanoSIMS (Polerecky et al. 2012), which allows a user to hand-draw regions of interest (ROIs) corresponding to different organelles (e.g., dinoflagellate starch grains, foraminiferal lipid droplets, and fibrillar bodies). For each type of organelle and each timepoint, the average ^{13}C-enrichment and its standard deviation were calculated based on three replicate foraminifera (except for the 6 and 30 h timepoints, where only two replicates were available). The ROIs drawn on TEM images were also used to assess the relative abundance (in %) of lipid droplets in the foraminiferal endoplasm and starch grains in the dinoflagellate cytoplasm, respectively. Lipid droplet abundance was determined as the number of pixels occupied by lipid droplets divided by the total number of pixels of foraminiferal endoplasm. Starch grain abundance was determined as the number of pixels of occupied by starch grains divided by the total number of pixels covering dinoflagellate cytoplasm.

We recognize that chemical fixation protocols are known to affect the ^{13}C-content of cells, through

infiltration of ^{12}C-resin and fixatives within the samples and loss of soluble ^{13}C-enriched compounds (Musat et al. 2014; Nomaki et al. 2018). Thus, the ^{13}C-enrichment values of the different cellular compartments (including the starch grains) noted in this study are not the original enrichments values. However, with all specimens prepared for NanoSIMS analysis in a similar manner, relative comparisons can be made.

Statistical analysis

Starch abundances in dinoflagellates, lipid droplet abundance in foraminiferal endoplasm, as well as dinoflagellate starch, and foraminiferal lipid δ^{13}C, were obtained by calculating the average of ROIs (one ROI corresponding to one organelle, i.e., a starch grain or, a lipid droplet) within each specimen, and then calculating the average of the three specimens for each timepoint. Thus, the errors bars shown are standard deviations representing the inter-specimen variability (i.e., $n=3$ specimens). However, statistical analysis was also carried out on the total set of ROIs for each timepoint using a linear mixed-effects (LME) model taking into account pseudo-replication effects, followed by a Tukey multiple comparison test. The results of the Tukey multiple comparisons tests are provided in the Online Resource 2. Comparisons of relative starch abundance and δ^{13}C in dinoflagellate endoplasm or matrix were performed with a *t* test for each timepoint. The results of the *t* tests are listed in the Online Resource 3. All statistical analyses were performed with the Rstudio software (RStudio Team 2016) with the significance level set to $\alpha=0.05$ (i.e., p value <0.05).

Results

The partitioned distribution of the cytoplasm into endo- and ectoplasm is easily observable in histological (semi-thin) section images, as illustrated with two specimens of *O. universa* (Fig. 2C, D). A few specimens grew a chamber during the experiment (Online Resource 4); those have a spherical test surrounding a multi-chambered trochospiral test. The trochospiral test chamber is filled with cytoplasm (=endoplasm), and although the space between the trochospiral test and the spherical test appears empty, it originally contained strands of rhizopodia and seawater (Spero 1988) that were washed away and replaced by resin during the fixation process. We refer to the space between the trochospiral test and spherical chambers as the 'internal matrix' (im), to distinguish it from the 'external matrix' (em), defined here as the ectoplasm outside the spherical chamber (Fig. 2C, D). For the majority of the specimens that did not produce a spherical test prior to fixation, distinction is simply made between endoplasm (ep) and ectoplasmic matrix outside the trochospiral test. As we have no data to help elucidate, in this study, we assumed that there is no influence of calcification on the inorganic carbon assimilation in *O. universa*.

Dinoflagellate migration in and out of the foraminiferal endoplasm

As reported previously (Hemleben et al. 1985), we observed a diurnal migration pattern in the symbiotic dinoflagellates. In the light, the majority of symbiotic dinoflagellates were located on the spine surfaces surrounding the foraminifera test (i.e., in the external matrix) (Fig. 2A, C). However, a small subset of the dinoflagellate population was observed in the internal matrix and in vacuoles in the endoplasm (Fig. 2C, E). In contrast, symbionts were absent from the spines and ectoplasm at night (Fig. 2B, D), and were nearly all found in vacuoles within the endoplasm (Fig. 2F), although a few were observed in the internal matrix in the case of adult specimens. TEM and light micrographs of individuals fixed during day and night suggest that there is a permanent, albeit fluctuating, population of dinoflagellates in the endoplasm (Fig. 2E, F).

Carbon uptake and storage by the symbiotic dinoflagellates

Starch is the primary form of carbon storage in the dinoflagellates (Taylor 1968; Dodge and Crawford 1971). In TEM images, this carbohydrate appears as an electron transparent, white region in cells (e.g., Dodge and Crawford 1971; Spero 1987). After 45 min of incubation in spiked seawater, we see evidence of ^{13}C-enriched starch accumulation on the chloroplast pyrenoid surfaces (Fig. 3). Within 2 h, we observe a number of isolated starch grains within the cytosol, suggesting that the dinoflagellates harvest accumulating starch off the pyrenoid. TEM micrographs of dinoflagellates fixed at the end of the pulse light phase (i.e., after 6 h) display a higher starch grain density compared to earlier timepoints (Figs. 3 and 4A). Conversely, at the end of the night cycle ($T=18$; following 12 h of chase phase), TEM micrographs reveal nearly starch-free dinoflagellates (Fig. 4B).

We do not observe significant differences in starch relative abundance or average ^{13}C-enrichment between dinoflagellates in the endoplasm and those in the external matrix (*t* test, p value >0.05; Fig. 4C, D), indicating comparable photosynthetic efficiency and equal access to $^{13}CO_2$. The relative abundance of starch grains in all dinoflagellates (expressed in percentage of the area occupied by starch grains) increased from ~11% after 45 min to ~43% after 6 h of incubation in the light (LME model, p value <0.001; Fig. 4C). During the dark phase, the starch relative abundance stayed constant between 6 and 7 h of incubation (LME model, p value >0.05), and decreased steadily to ~7%

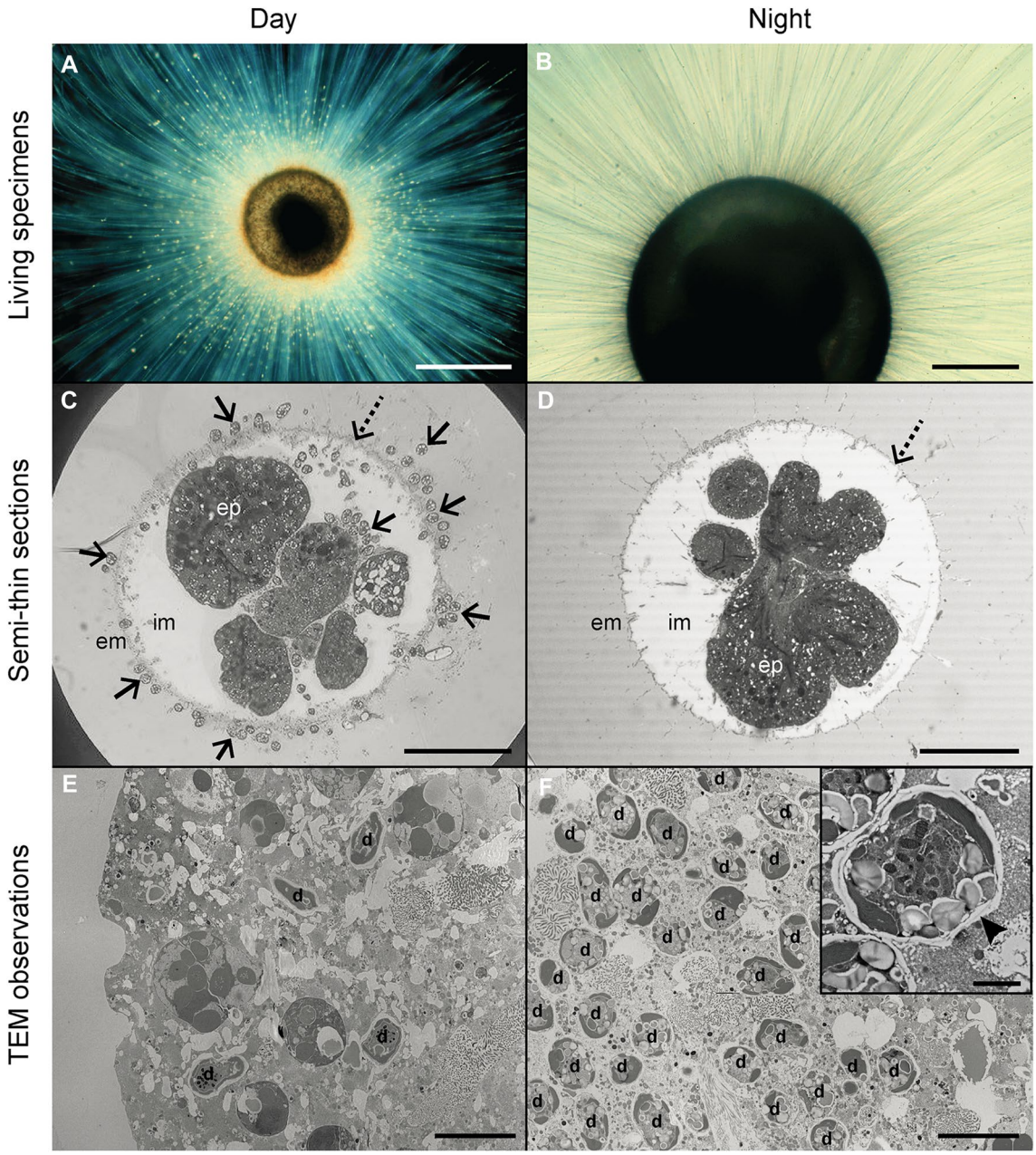

Fig. 2 *Orbulina universa* during day ($t = 2$ h; left column) and night ($t = 12$ h; right column). Light micrographs of living specimens (**A**, **B**), semi-thin sections (**C**, **D**), and TEM micrographs of the cytoplasm with dinoflagellate symbionts (d) in vacuoles within the *O. universa* endoplasm (**E**, **F**). During the day, the majority of the symbionts are outside the spherical test on the spines (yellow dots in **A**). Symbionts are evident outside the sphere in the external matrix (em) in **C**, with a few symbionts observed in the internal matrix (im) (**C**). A few symbionts are found in the endoplasm (ep) during the day (**E**). During the night, symbionts are absent from the spines (**B**). At this time, they are primarily found in the endoplasm (ep) (**D**, **F**). A vacuole membrane surrounding a dinoflagellate symbiont is clearly visible inside the foraminiferal endoplasm (inset in **F**, indicated by an arrowhead). Dotted arrows in **C**, **D** point to the position of the original (decalcified) spherical test. Dinoflagellates are indicated with solid arrows or labeled 'd'. Scale bars: **A** 500 µm; **B**–**D** 200 µm; **E**, **F** 10 µm; inset in **F** 2 µm

during the remainder of the dark phase, i.e., $T = 18$ h of incubation (LME model, p value < 0.001). During the second light phase (from $T = 18$ h to $T = 30$ h), starch abundance again increased to an average of ~41% of the symbiont cytosol area (LME model, p value < 0.001; Fig. 4C).

^{13}C-enrichment of the starch was evident after 45 min in seawater with ^{13}C-labeled bicarbonate (Fig. 3; 45 min). Mean starch δ^{13}C in the dinoflagellates increased by about a factor of 4, from ~3400 to ~13,200‰ between ($t = 45$ min) and the end of the light pulse phase ($t = 6$ h)

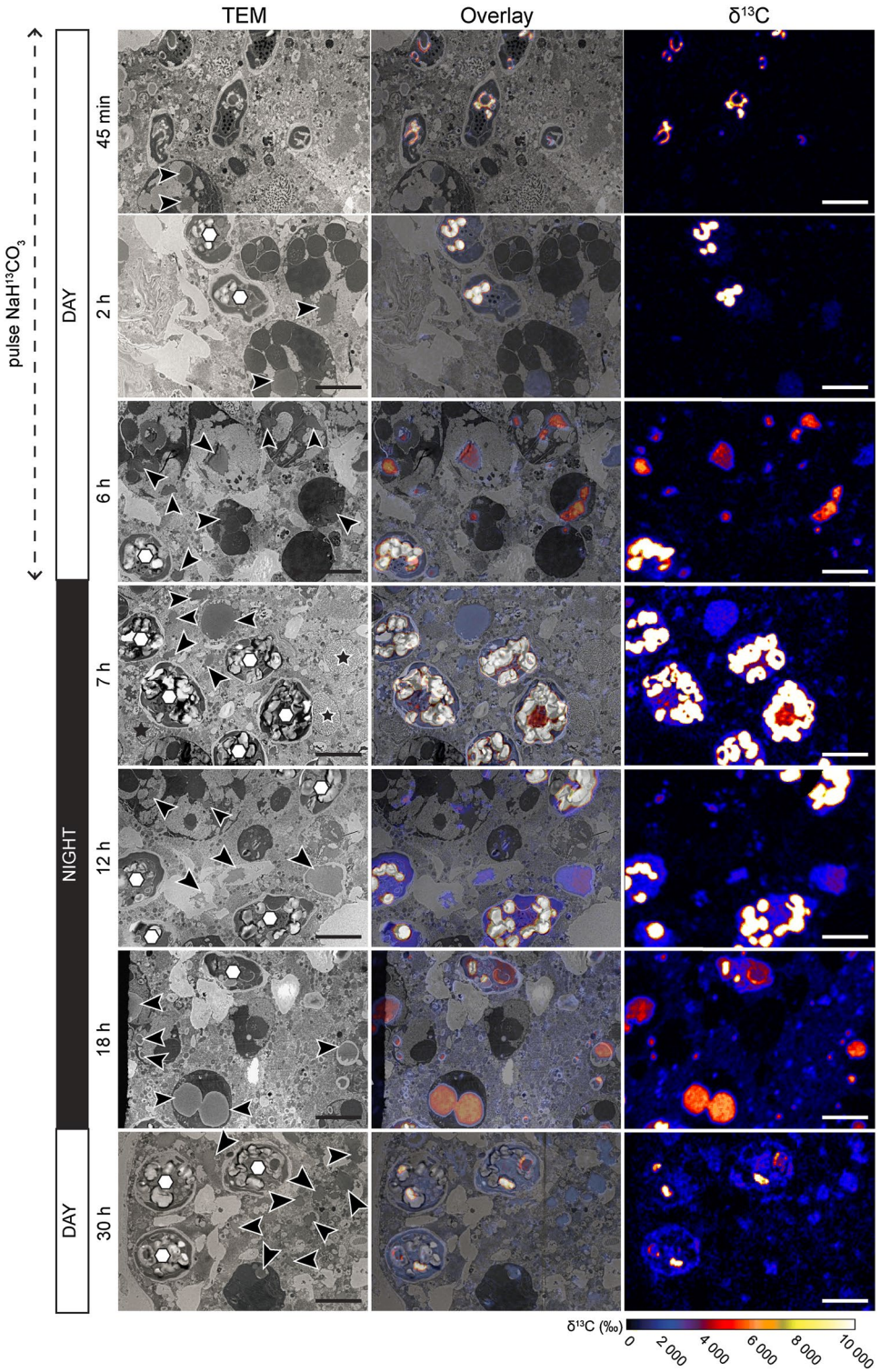

Fig. 3 Time evolution of starch production and ^{13}C incorporation by the symbiotic dinoflagellates in *Orbulina universa* endoplasm during the daytime pulse phase of the experiment (45 min, 2 h, 6 h), followed by a night ($T = 7$ h, 12 h, 18 h) and second light cycle ($T = 30$ h) chase phase. Left column: TEM micrographs of *O. universa* endoplasm with symbiotic dinoflagellates. Right column: corresponding NanoSIMS images of $^{13}C/^{12}C$ distributions (expressed as $\delta^{13}C$ in ‰). Central column: overlay of the TEM and NanoSIMS images. Black arrowheads: foraminiferal endoplasm lipid droplets. White hexagons: symbiotic dinoflagellates. Black stars: fibrillar bodies. Objects appearing white in NanoSIMS images are starch deposits with ^{13}C-enrichments above the imposed 10.000‰ upper color scale limit. Scale bars: 5 µm

(LME model, p value < 0.001; Fig. 4D). In the subsequent dark chase phase ($t = 6$ to 18 h), dinoflagellate starch ^{13}C-enrichment remained constant (LME model, p value > 0.05), albeit with a tendency to decrease towards the end of the night. During the subsequent light chase phase ($t = 18$–30 h), unlabeled starch accumulated (Fig. 4C) and the average dinoflagellate starch ^{13}C-enrichment decreased to ~ 1200‰ (LME model, p value $= 0.001$; Fig. 4D).

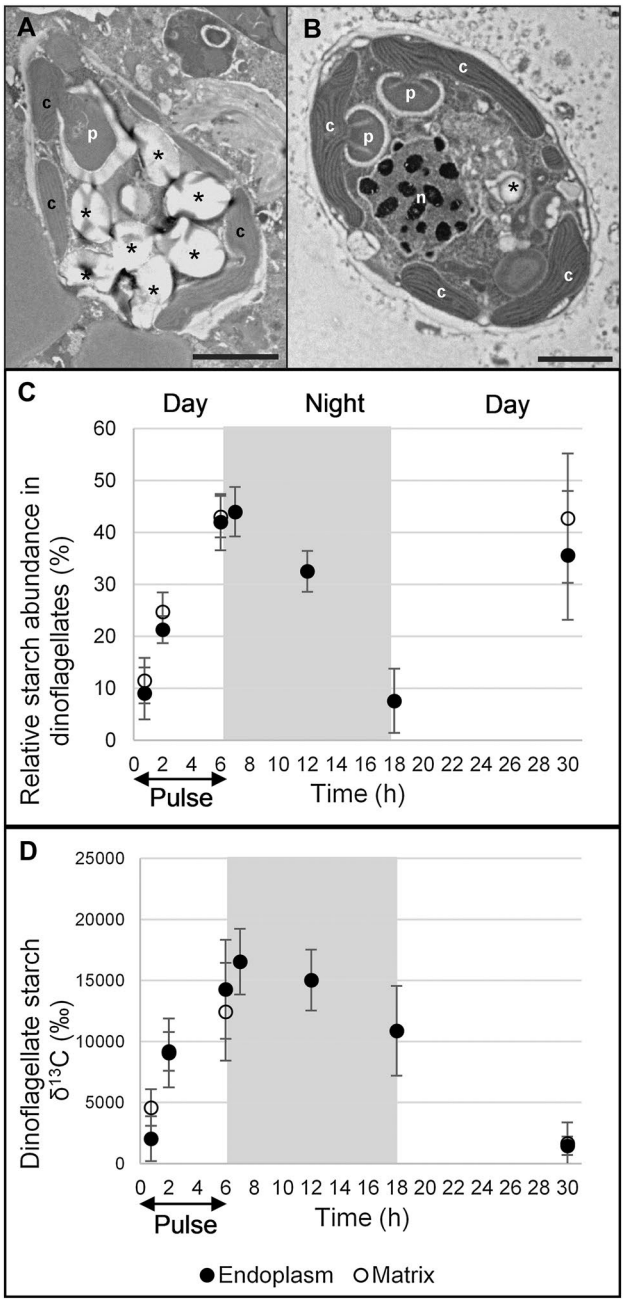

Fig. 4 Dinoflagellate starch grain abundances and their ^{13}C-enrichments. TEM micrographs of dinoflagellates in the endoplasm of *O. universa* illustrating the difference in starch grain content between the end of the day (**A**) and after 12 h in darkness (**B**). Asterisks: dinoflagellate starch grains, c: dinoflagellate chloroplasts, n: dinoflagellate nucleus, p: pyrenoids. Scale bars: 2 µm. **C** The relative abundance of starch grains in dinoflagellates (in % of total cytoplasm area). **D** Average starch ^{13}C-enrichments. A distinction is made between starch from dinoflagellates present in the endoplasm (black circles) or in the internal/ectoplasmic matrix (white circles) of *O. universa*. Error bars: ± 1 SD ($n = 3$ specimens)

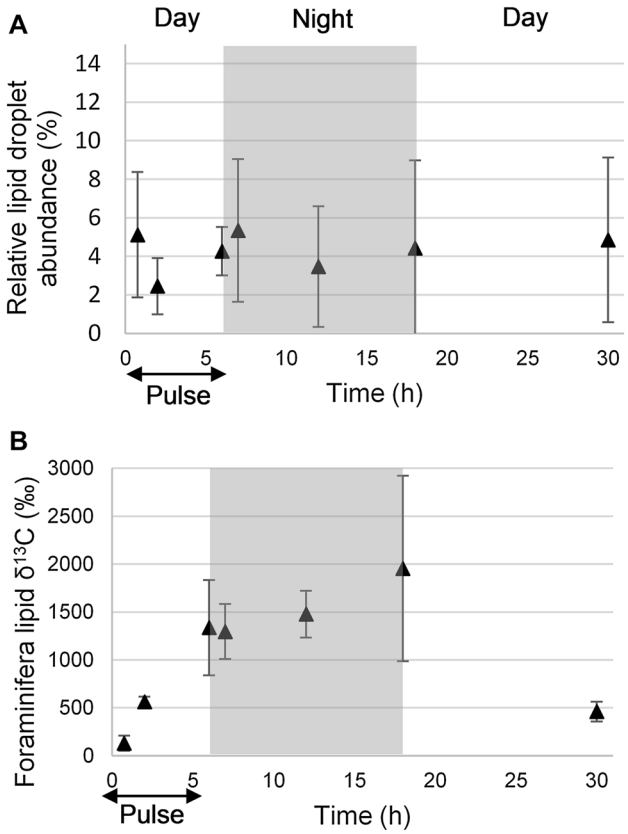

Fig. 5 Lipid droplet relative abundance and average ^{13}C-enrichment in *O. universa* endoplasm as a function of time. Error bars: ± 1 SD ($n = 3$ specimens)

Transfer of carbon to the foraminiferal host cell

The first evidence of translocation of ^{13}C-enriched photosynthates from symbiont to foraminifera host was recorded by a statistically significant increase in ^{13}C-labeled lipid droplets at the first timepoint ($t = 45$ min) (Figs. 3 and 5B). Lipid droplets are osmiophilic vesicles in the cell (i.e., they appear electron dense in TEM images) with a waxy appearance and without apparent membrane (reviewed in LeKieffre et al. 2018). They are thought to be one of the primary carbon storage components in foraminiferal cells (Hottinger and Dreher 1974; Leutenegger 1977). Host lipid droplets have an average δ^{13}C of ~ 100‰ at $T = 45$ min, which increased to ~ 2000‰ at $T = 18$ h (LME model, p value < 0.001; Fig. 5B) before significantly decreasing to ~ 450‰ at the end of the second light phase (LME model, p value < 0.01; Fig. 5B). Although δ^{13}C of the lipid changed across the experimental time period, the relative abundance of lipid droplets within the foraminiferal cell remained constant at ~ 5% during the entire experiment (LME model, p value > 0.05, Fig. 5A).

During the initial 18 h of the experiment (6 h pulse + first night chase period), the foraminiferal endoplasm background underwent a slow, spatially heterogeneous increase

in ^{13}C that is particularly evident at the end of the night chase phase ($T = 18$ h; Fig. 3). Higher magnification TEM and NanoSIMS images of specimens fixed during the dark chase phase revealed small (0.2–1 µm) ^{13}C-enriched lipid droplets within the host cytoplasm after 12 h of incubation (Fig. 6A). These lipids were often observed in direct contact or extremely close to the symbiosome membranes surrounding the dinoflagellates, as well as within the symbiont adjacent to the symbiosome membrane (Fig. 6).

High-magnification TEM and NanoSIMS images also reveal small (0.2–0.5 µm diameter), spherical to irregularly shaped electron-opaque structures (nature and function unknown) that are enriched in ^{13}C and distributed evenly throughout the foraminiferal endoplasm (Fig. 7A, B). In addition, some fibrillar bodies (Lee et al. 1965) exhibit high δ^{13}C values, whereas adjacent fibrillar bodies were not significantly enriched in ^{13}C (Fig. 7C, D), possibly indicating different stages and timing of development with respect to the pulse phase period.

Dinoflagellate cell division within the foraminiferal host cell

Dividing cells are only observed during the night period when mitosis produces dinoflagellate cells with two nuclei composed of condensed chromosomes (Fig. 8A). At the start of the night phase, prior to mitosis, ^{13}C-enrichments is primarily observed in starch C (Fig. 8B, C). At the end of the night phase ($T = 18$ h), following symbiont mitosis, the ^{13}C-enrichment in the

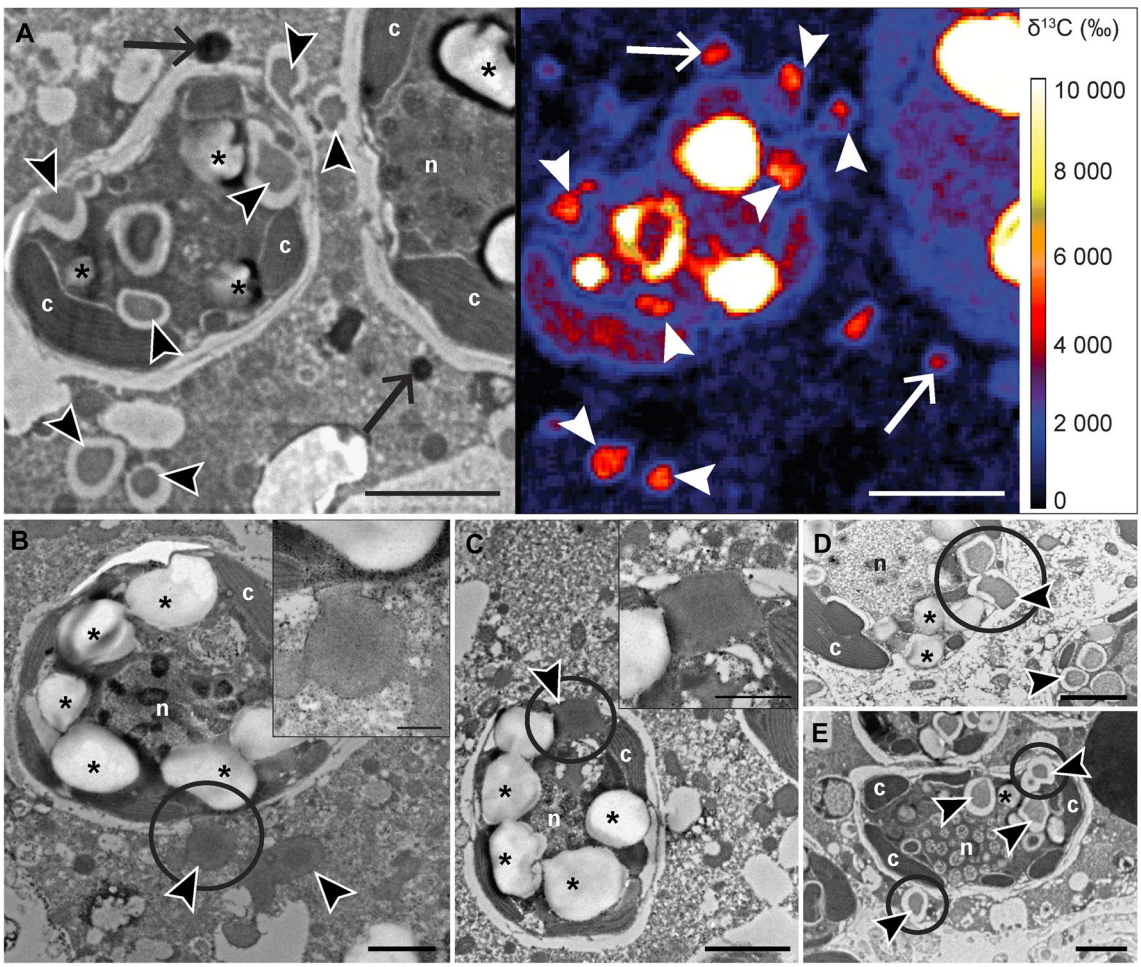

Fig. 6 Inferred translocation of ^{13}C-enriched lipids from the symbiotic dinoflagellates to *O. universa* endoplasm. **A** TEM micrograph and corresponding NanoSIMS image showing the ^{13}C-enrichment of the lipid droplets observed within a dinoflagellate and within the foraminiferal endoplasm at $T = 12$ h. **B**–**E** TEM micrographs of dinoflagellates in *O. universa* endoplasm during the night phase at $T = 12$ h. Circles are drawn around potential lipid transfer areas from the dinoflagellate to the foraminiferal endoplasm, i.e., lipid droplets, either in very close proximity or in direct contact with the symbiosome membrane. In some specimens, lipid droplets have a void around the lipid core, which is likely an artifact of the fixation process. Insets in **B** and **C** show higher magnification images of the potential lipid transfer circled in **B** and **C** micrographs. Arrowheads: lipid droplets, arrows: electron-opaque bodies, asterisks: dinoflagellate starch grains, c: dinoflagellate chloroplasts, n: dinoflagellate nucleus. Scale bars: **A**, **C**–**E** 2 µm; **B**, inset **D** 1 µm; inset **B** 500 nm

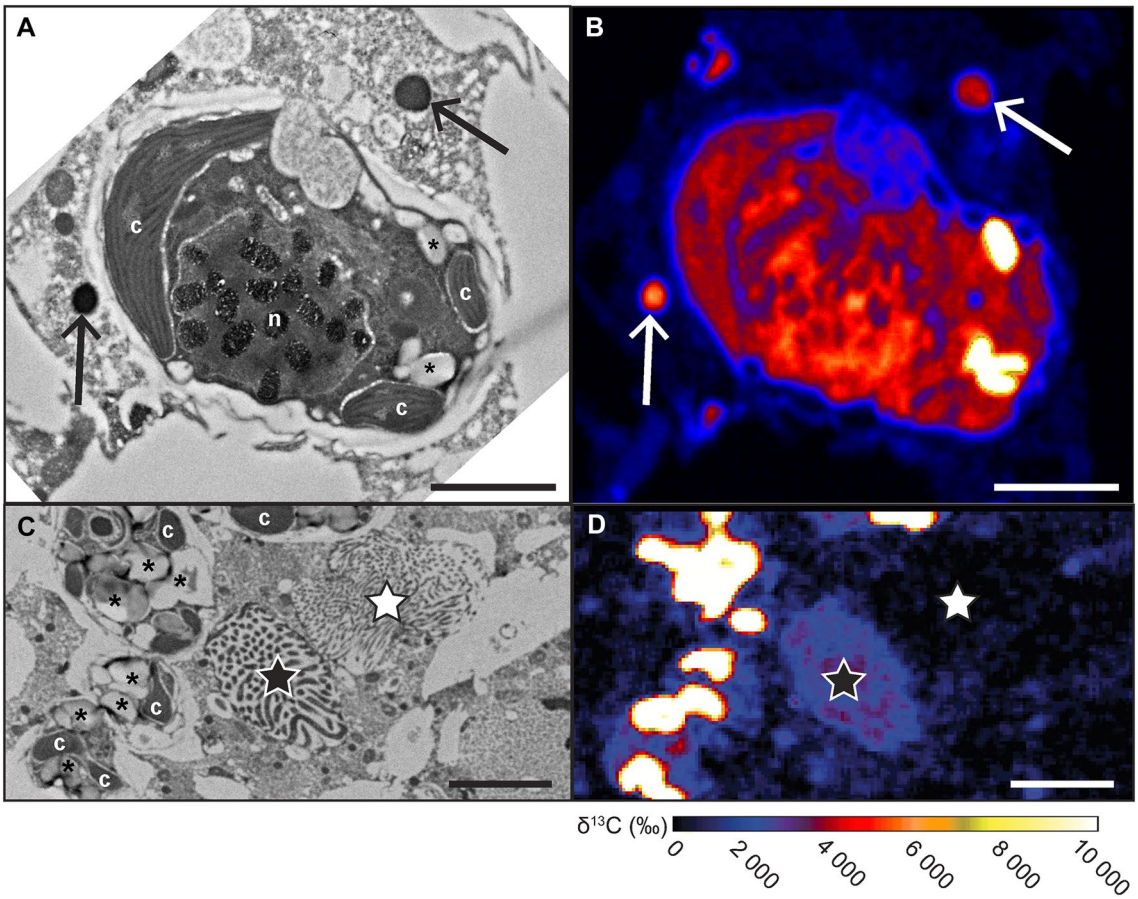

Fig. 7 ^{13}C-enriched electron-opaque and fibrillar bodies. Left: TEM micrograph. Right: Corresponding NanoSIMS image. **A**, **B** ^{13}C-enriched electron-opaque bodies in close proximity to a symbiotic dinoflagellate. Adjacent fibrillar bodies in the *O. universa* endoplasm at $T = 12$ h of incubation (i.e., after 6 h in light with ^{13}C-enriched bicarbonate and 6 h in dark with normal seawater): one is ^{13}C-enriched (black star), while the other is not (white star). Arrows: electron-opaque bodies, asterisks: dinoflagellate starch grains, stars: fibrillar bodies, c: dinoflagellate chloroplasts, n: dinoflagellate nucleus. Scale bars: **A**, **B** 2 µm; **C**, **D** 5 µm

dinoflagellates is more evenly distributed, with clear ^{13}C-enrichment in the nucleus and chloroplasts (Fig. 8D, E). This demonstrates that carbon fixed during the previous day is utilized for both dinoflagellate cell division and foraminifera growth.

Dark incubation

When foraminifera and their symbiotic dinoflagellates are incubated in the dark for 6 h in ^{13}C-spiked ASW, the cells do not display a ^{13}C-enrichment in either the symbiont starch granules or foraminifera endoplasm (Online Resource 5). Although lipid droplets were also observed in the foraminiferal endoplasm they showed no sign of ^{13}C-enrichment either. These results confirm that the primary pathways for cellular carbon in the foraminifera–symbiont system are through symbiont photosynthesis.

Discussion

Diurnal patterns of symbiont distribution

As previously documented in other symbiotic planktic species (Anderson and Bé 1976; Bé and Hutson 1977) and in *O. universa* (Bé et al. 1977; Spero 1987), dinoflagellate symbionts move along the foraminiferal spines, synchronized to the day–night cycle (Fig. 2). At the onset of darkness, these dinoflagellates migrate down the spines, pass through the juvenile chamber apertures, and are incorporated into membrane bound vacuoles (symbiosomes) within the foraminifera endoplasm. During the day, this process reverses. However, we observed a small number of symbionts remaining within the endoplasm of *O. universa* during the day. Anderson and Bé (1976) suggested that by keeping a daytime sub-population of dinoflagellates within their endoplasm, the foraminifera could enhance transfer of photosynthates to the host. Indeed, in our study,

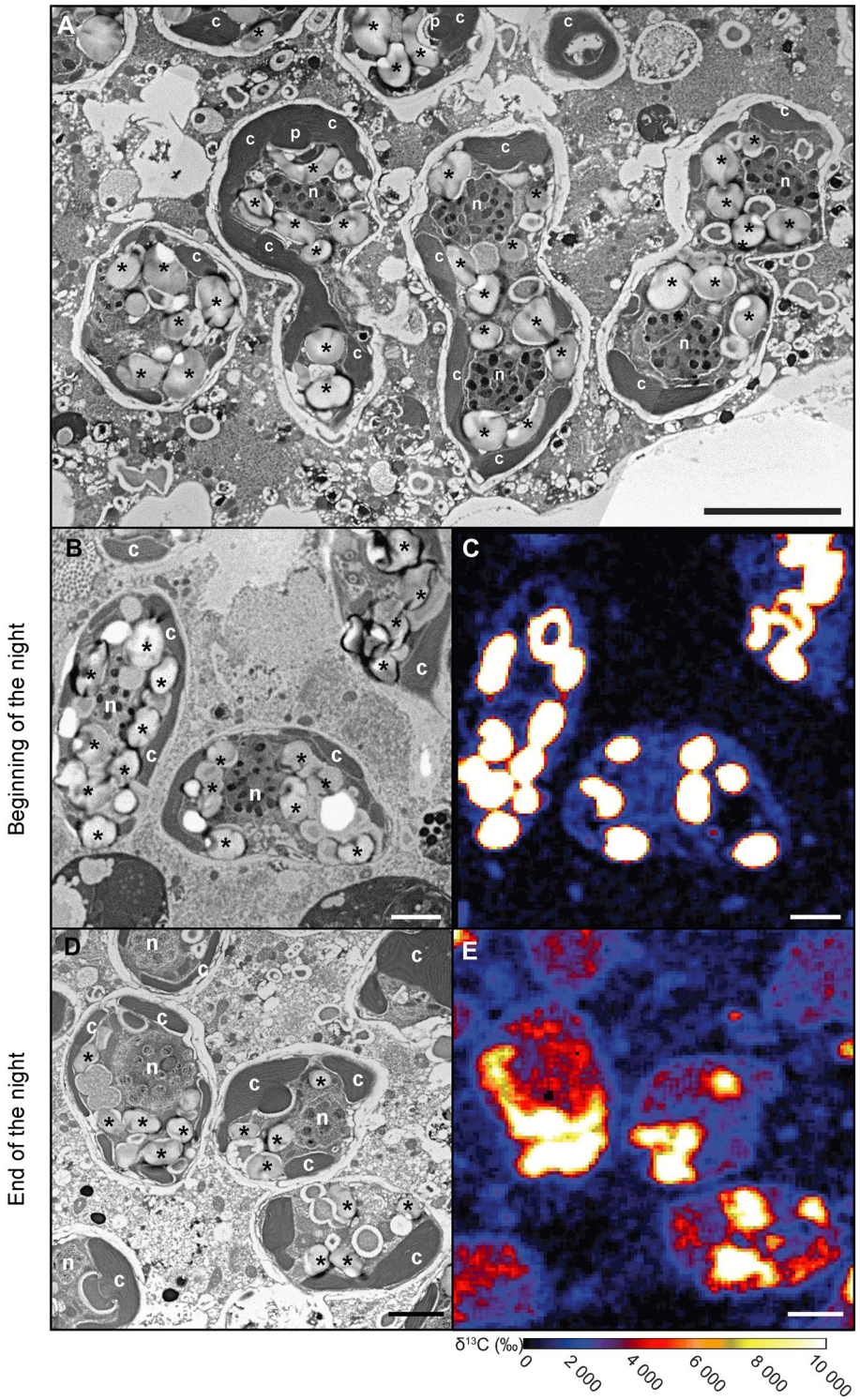

Fig. 8 Dinoflagellate mitosis. **A** TEM micrograph of three dinoflagellate symbionts undergoing mitosis in the *O. universa* endoplasm at $T = 12$ h (i.e., middle of the night phase; cf. Fig. 1). TEM micrographs (**B**, **D**) and corresponding NanoSIMS ^{13}C-enrichment images of dinoflagellates in *O. universa* endoplasm at the beginning of the night (**C**) and at end of the night (**E**), respectively. Asterisks: Dinoflagellate starch grains, c: dinoflagellate chloroplasts, n: dinoflagellate nucleus, p: dinoflagellate pyrenoids. Scale bars: **A** 5 µm; **B**–**E** 2 µm

evidence of translocation of ^{13}C-enriched photosynthates from symbiont to foraminifera lipid droplets is seen during the light phase (Figs. 3 and 5B), suggesting that the symbiont population is providing the foraminifera with assimilated carbon at all times throughout a 24 h period (Fig. 9).

Photosynthate assimilation and turnover in the symbiotic dinoflagellates

Oxygen flux measurements using micro-sensors in *O. universa* have demonstrated efficient O_2 production by the dinoflagellate photosynthetic system, and hence efficient

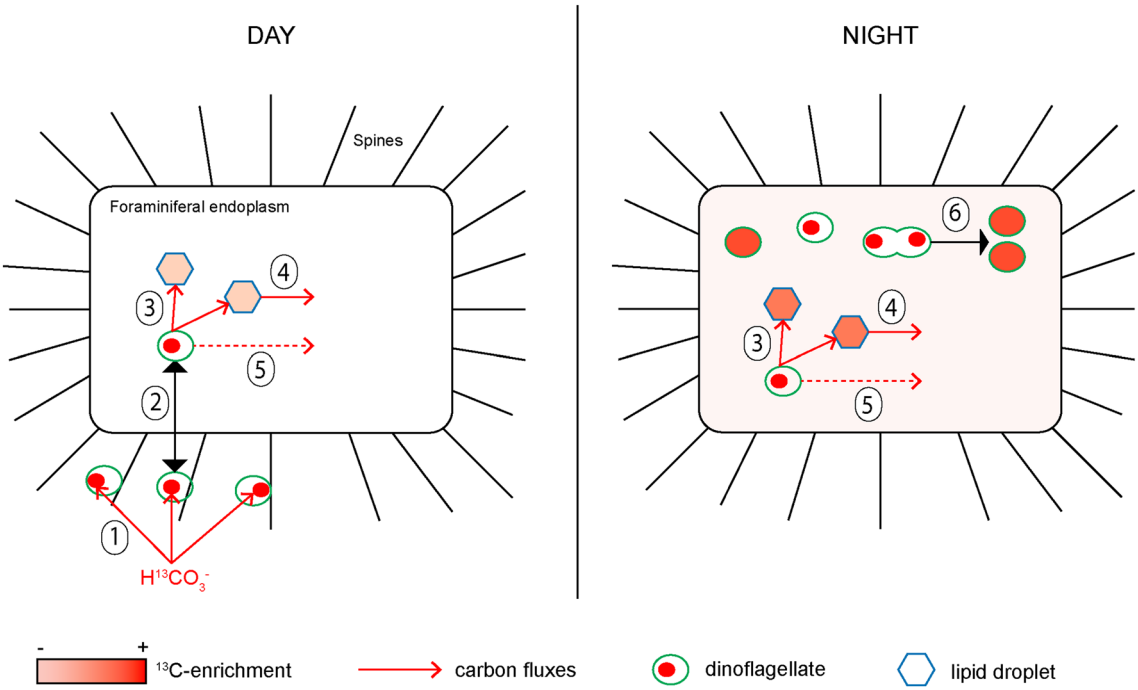

Fig. 9 Schematic diagram of the carbon assimilation pathway in the symbiotic association of *Orbulina universa* and photosynthetic dinoflagellates. (1) During day, the inorganic carbon from the ambient seawater is assimilated by the dinoflagellates via photosynthesis and accumulated in their starch grains. (2) Although the majority of the dinoflagellates are on the spines, some migrate in the foraminiferal endoplasm. (3) A part of the dinoflagellate ^{13}C-photosynthates is transferred during the day to the foraminiferal lipid droplets. (4) ^{13}C-enriched fatty acids of the foraminiferal lipid droplets are transferred to the foraminiferal endoplasm to be available for metabolic processes. (5) A concomitant transfer of ^{13}C-rich soluble compounds from the dinoflagellates to the foraminiferal endoplasm is also possible. (3–5) The transfer of ^{13}C-rich compounds from the dinoflagellates into host lipid droplets and from the lipid droplets to the foraminiferal endoplasm, continue during the night. In parallel, the symbiotic dinoflagellates undergo mitosis (6), resulting in the formation of more homogeneously ^{13}C-enriched dinoflagellates

photosynthetic C-fixation (Jørgensen et al. 1985; Rink et al. 1998; Köhler-Rink and Kühl 2005). Starch, which is the most abundant photosynthetic C storage form in plant cells, consists of amylopectin and amylose synthesized from glucose (supplied by photosynthetic C-fixation), and its degradation results mainly in the formation of glucose and maltose, which can be further processed to other C compounds (Preiss 1982; Smith et al. 1997; Zeeman et al. 2010). In symbiotic dinoflagellates, starch is also the main form of carbon storage, followed by lipid droplets (Taylor 1968; Dodge and Crawford 1971).

The incorporation of ^{13}C into starch on the dinoflagellate pyrenoid surfaces was evident after only 45 min in the ^{13}C pulse (Fig. 3), and most likely started as soon as the symbiont was exposed to light (Fig. 4D). Subsequent transfer of starch from the pyrenoid surface to the dinoflagellate cytosol, in addition to the continuous increase in starch grain density throughout the first light pulse phase, has never been observed in this symbiotic system (Fig. 3). However, corals exposed to a comparable ^{13}C pulse-chase experiment exhibited similar carbon uptake timing and starch storage in the symbiotic dinoflagellate *Symbiodinium* spp. (Kopp et al. 2015b). During the night phase (Fig. 4C), starch density decreases continuously, likely due to a combination of dinoflagellate respiration, cell division (as indicated by ^{13}C redistribution to other dinoflagellate organelles following mitosis; Fig. 8E), as well as photosynthate translocation to the host (Figs. 3, 5, and 6).

Photosynthate translocation inside the host cell

In cnidarian symbiosis, translocation of photosynthates have been observed in the form of glycerol, glucose (or other hexoses), amino acids, or lipids (Muscatine et al. 1967; Trench 1971, 1979; Hofmann and Kremer 1981; Kellogg and Patton 1983; Patton and Burris 1983; Whitehead 2003). Because the sample preparation we use for TEM–NanoSIMS analysis does not preserve soluble compounds (Nomaki et al. 2018; Nuñez et al. 2018), our study does not reveal information on the transfer of soluble photosynthates, such as glycerol, hexoses, and amino acids in the *O. universa* symbiotic system. However, lipids are largely preserved during sample preparation and can be studied.

The absence of ^{13}C-enrichment in the foraminiferal lipid droplets and endoplasm of specimens incubated 6 h in the dark (Online Resource 5) suggests that *O. universa* does not possess its own pathway for inorganic carbon assimilation. Thus, we conclude that the ^{13}C-enrichment observed in the foraminiferal endoplasm, including the lipid droplets, incubated in the light was the result of a photosynthetic process, acquired through the symbiosis with photosynthetic dinoflagellates.

After 45 min of incubation, we observe ^{13}C-enriched lipid droplets within the foraminiferal endoplasm (Fig. 3), indicating rapid translocation of ^{13}C-photosynthates from the dinoflagellate to the foraminiferal host cell. Fast C transfer was also observed in a coral symbiotic system, where ^{13}C-enriched host lipids were observed after only 15 min (Kopp et al. 2015b). The increase of lipid ^{13}C-enrichment during the first 18 h of this experiment (Fig. 5) suggests that photosynthate carbon is translocated between the dinoflagellates and foraminiferal host continuously during day and night. In addition, the observed gradual increase in ^{13}C-enrichment of all foraminiferal endoplasm compartments (Fig. 3) suggests that translocated photosynthate carbon is closely coupled to the foraminifera anabolic needs.

The relative abundance of lipid droplets in the *O. universa* endoplasm did not vary during the experiment (Fig. 5A). This observation suggests the rates of lipid production, C translocation, and lipid utilization by the host cell is at equilibrium. The decrease in foraminiferal lipid droplet ^{13}C-enrichment during the chase phase (Fig. 5B) indicates that the lipid droplet content was both utilized by foraminiferal metabolism and renewed by lipids not labeled with ^{13}C. The former results in a spatially heterogeneous ^{13}C-enrichment of the foraminiferal endoplasm that we observe in the pulse phase of our experiment (Fig. 3). However, we cannot exclude the possibility of a direct transfer of soluble compounds from the dinoflagellates to the foraminiferal endoplasm for foraminiferal metabolic needs (Fig. 9).

The implications of soluble compound C transfer from symbiotic microalgae to host have been reported previously in the literature. For example, in the symbiotic radiolarian *Collosphera huxleyi*, and the coral *Heteroxenia fuscescens*, C transfer between photosynthetic symbiont and the host cell is thought to involve a glycerol transfer step prior to the production of lipids (e.g., wax, fatty acids, and triglycerides) (Anderson et al. 1983; Schlichter et al. 1983). In *H. fuscescens*, Schlichter et al. (1983) reported a rapid conversion of soluble compounds into lipids in both symbiont and host cells. The reprocessing of soluble C compounds was also shown in the coral *Acropora* cf. *scandens*, in which labeled ^{14}C-glycerol and ^{14}C-glucose were rapidly converted into lipids. After 60 min of incubation, ~ 30% of the ^{14}C fraction was found in the lipophilic fraction (Schmitz and Kremer 1977). However, the authors could not determine whether the reprocessing of the photosynthates occurred in the symbionts or in the host. Transfer of lipid and soluble compounds might be concomitant in the symbiosis between dinoflagellates and foraminiferal cells. In cnidarians, these transfer processes are controlled by the host through the expression of specific molecules to stimulate or inhibit the release of photosynthates from the algae (Yellowlees et al. 2008). Thus, depending on the environmental conditions and the host metabolic state, the host could modulate this transfer and preferentially trigger the translocation of lipids or soluble compounds. Although the pathway(s) for lipid synthesis and transfer between symbiont and host in *O. universa* remain to be determined, it is clear that lipids play an important role in C cycling in this organism. The observation of ^{13}C-enriched lipid droplets in direct contact with (and on either side of) the symbiosomes (Fig. 6) might indicate that lipids are transferred across this membrane by the process of exocytosis, although we have made no direct observations to prove this hypothesis.

Production and accumulation of lipid droplets in the *O. universa-dinoflagellate* symbiotic system raise the intriguing possibility that lipid production could also be intimately related to buoyancy control. Spero (1988) noted that the majority of *O. universa* specimens studied in the laboratory produce their spherical chambers late at night when the symbionts are sequestered within the endoplasm. Production of a large final chamber, coupled with chamber thickening during calcification (Spero 1988), requires a mechanism to generate positive buoyancy to quickly counter the density increase of the organism that is associated with calcification. We hypothesize that lipid production associated with C translocation plays a significant role in this buoyancy control (Caromel et al. 2014). Such a function for lipids could provide a rationale for the observed baseline lipid levels in the foraminifera cells a well as to justify the type of C translocated between symbiont and host cell, i.e., lipid versus soluble C, as discussed above.

A number of additional ^{13}C-enriched structures are seen in the TEM images. For instance, small ^{13}C-enriched, electron opaque, spheres observed in the foraminiferal endoplasm (Figs. 6A and 7) likely correspond to the electron-opaque bodies (also called "electron-dense bodies" or "osmiophilic granules") described in both benthic and planktic foraminifera (Leutenegger 1977; Nomaki et al. 2016; LeKieffre et al. 2018). Such structures appear in TEM micrographs of planktic species in the previous publications (Anderson and Bé 1976; Hemleben et al. 1989). These electron-opaque bodies are known to contain nitrogen and significantly more sulfur than other organelles, but their function remains unknown (Nomaki et al. 2016).

Another organelle that is unique to planktic foraminifera, fibrillar bodies (Fig. 7), is observed in the *O. universa* endoplasm. These structures were previously described in

light microscopic and TEM studies of different planktic species (Lee et al. 1965; Hansen 1975; Anderson and Bé 1976; Spero 1988; Anderson and Lee 1991). The observation that some fibrillar bodies are enriched in ^{13}C, whereas other such organelles lack ^{13}C enrichment suggests that the population of fibrillar bodies we observe in micrographs formed both prior to and during the pulse phase of our experiment. Based on cytological staining, Lee et al. (1965) showed that fibrillar bodies are rich in proteins. Although the role of this organelle is still controversial, Spero (1988) presented TEM evidence that suggests fibrillar body proteins play a role in organic matrix formation during chamber biomineralization.

Dinoflagellate photosynthesis and mitosis: the role of the host?

During the night chase phase of our experiments (i.e., between $T = 12–18$ h), the vacuolized dinoflagellates residing in the endoplasm were frequently observed undergoing mitosis (Fig. 8). No dinoflagellates were observed undergoing cell division during light periods. Furthermore, photosynthetically assimilated ^{13}C-enriched carbon was a major contributor to the anabolic processes taking place during mitosis (Fig. 8). This timing of mitosis requires explanation. It has been suggested that the foraminiferal endoplasm is the most favorable environment for symbiont reproduction (Faber et al. 1988) because of greater availability of nutrients (such as N and P) obtained via prey capture (Jørgensen et al. 1985). Studies with diatoms and dinoflagellates in culture have shown that a pulse of nutrients can induce cell division of the microalgae (Doyle and Poore 1974). Symbiotic dinoflagellates of the pelagic cnidarian *Mastigias* sp. undergo mitosis at night when the host is visiting the nutrient-rich chemocline lower in the water column (Wilkerson et al. 1983). Because *O. universa* typically inhabits low-nutrient environments (Spero and Parker 1985), it might be necessary for the symbiotic dinoflagellates to migrate into an environment (i.e., the endoplasm) rich in N and P to trigger mitosis (Uhle et al. 1999). Jørgensen et al. (1985) showed, based on model calculations, that ambient N and P concentrations are insufficient to maintain the growth of the symbiotic dinoflagellates associated with the planktonic foraminifer *Globigerinoides sacculifer*; capture of prey by the foraminifer would be required to provide enough of these nutrients for dinoflagellate growth. Prey-capture experiments and experiments to elucidate the role of micro-nutrients, such as nitrates and ammonium, in mitosis would be interesting targets of future investigation.

Conclusion

By combining a ^{13}C-labeled bicarbonate pulse-chase experiment with correlated TEM and NanoSIMS imaging, we have traced the fate of C assimilation within the symbiotic association of planktic foraminifera and photosynthetic dinoflagellates (summarized in Fig. 9). Results show that dinoflagellates actively assimilate C into their starch grains during the day, and metabolize the fixed C by night via (1) respiration, (2) formation of new biomass supporting mitotic cell division, and (3) transfer to the foraminiferal cell. Carbon translocation is fast (< 45 min) and happens throughout a 24 h period, i.e., during day and night phases. The observation of lipid droplets in close association with the symbiosomes enclosing the dinoflagellates in the foraminiferal endoplasm indicates that lipids likely play an important role in this C transfer.

Data availability The data sets generated during and/or analyzed during the current study are available in the PANGAEA repository (https://doi.org/10.1594/pangaea.887995).

Acknowledgements We gratefully acknowledge the staff of the University of Southern California, Wrigley Marine Science Center for field and laboratory assistance. We thank Team Catalina 2014 (Tom Bergamaschi, Elisa Bonnin, Oscar Branson, Edward Chu, Kate Holland, Elliot Schoenig, and Jordan Snyder) for their skilled participation. The electron microscopy platform at the University of Lausanne (Switzerland) is thanked for expert advice and access to equipment. This collaboration was established by a chance meeting between the authors during a research visit to the Alfred Wegener Institute, Bremerhaven Germany, as part of a Humboldt Research award to HJS. We thank the Alexander von Humboldt Foundation for helping create this opportunity through its support. The work was supported by the Swiss National Science Foundation (Grant no. 200021_149333) and the US National Science Foundation (OCE-1261516). The authors declare that they have no conflict of interest. This article does not contain any studies with human participants or animals performed by any of the authors.

References

Anderson OR, Bé AWH (1976) The ultrastructure of a planktonic foraminifer, *Globigerinoides sacculifer* (Brady), and its symbiotic dinoflagellates. J Foraminifer Res 6:1–21. https://doi.org/10.2113/gsjfr.6.1.1

Anderson OR, Lee JJ (1991) Cytology and fine structure. In: Lee JJ (eds) Biology of foraminifera. Academic Press, London, pp 7–40

Anderson OR, Swanberg NR, Bennett P (1983) Assimilation of symbiont-derived photosynthates in some solitary and colonial radiolaria. Mar Biol 77:265–269

Bé AWH, Hutson WH (1977) Ecology of planktonic foraminifera and biogeographic patterns of life and fossil assemblages in the Indian Ocean. Micropaleontology 23:369. https://doi.org/10.2307/1485406

Bé AWH, Hemleben C, Anderson OR, Spindler M, Hacunda J, Tuntivate-Choy S, Be AWH (1977) Laboratory and field observations

of living planktonic foraminifera. Micropaleontology 23:155–179. https://doi.org/10.2307/1485330
Bé AWH, Spero HJ, Anderson OR (1982) Effects of symbiont elimination and reinfection on the life processes of the planktonic foraminifer *Globigerinoides sacculifer*. Mar Biol 70:73–86. https://doi.org/10.1007/BF00397298
Caromel AGM, Schmidt DN, Phillips JC, Rayfield EJ (2014) Hydrodynamic constraints on the evolution and ecology of planktic foraminifera. Mar Micropaleontol 106:69–78. https://doi.org/10.1016/j.marmicro.2014.01.002
Caron DA, Bé AW, Anderson OR (1981) Effects of variations in light intensity on life processes of the planktonic foraminifer *Globigerinoides sacculifer* in laboratory culture. J Mar Biol Assoc UK 62:435–451
Caron DA, Michaels AF, Swanberg NR, Howse FA (1995) Primary productivity by symbiont-bearing planktonic sarcodines (Acantharia, Radiolaria, Foraminifera) in surface waters near Bermuda. J Plankton Res 17:103–129
Ceh J, Kilburn MR, Cliff JB, Raina J-B, van Keulen M, Bourne DG (2013) Nutrient cycling in early coral life stages: *Pocillopora damicornis* larvae provide their algal symbiont (Symbiodinium) with nitrogen acquired from bacterial associates. Ecol Evol 3:2393–2400. https://doi.org/10.1002/ece3.642
Clode PL, Stern RA, Marshall AT (2007) Subcellular imaging of isotopically labeled carbon compounds in a biological sample by ion microprobe (NanoSIMS). Microsc Res Tech 70:220–229. https://doi.org/10.1002/jemt.20409
Dodge JD, Crawford RM (1971) A fine-structural survey of dinoflagellate pyrenoids and food-reserves. Bot J Linn Soc 64:105–115
Doyle RW, Poore RV (1974) Nutrient competition and division synchrony in phytoplankton. J Exp Mar Biol Ecol 14:201–210. https://doi.org/10.1016/0022-0981(74)90001-X
Duguay LE, Taylor DL (1978) Primary production and calcification by the soritid foraminifer *Archais angulatus* (Fichtel & Moll). J Eukaryot Microbiol 25:356–361
Faber WW, Anderson OR, Lindsey JL, Caron DA (1988) Algal-foraminiferal symbiosis in the planktonic foraminifer *Globigerinella aequilateralia*; I, Occurrence and stability of two mutually exclusive chrysophyte endosymbionts and their ultrastructure. J Foraminifer Res 18:334–343. https://doi.org/10.2113/gsjfr.18.4.334
Hansen HJ (1975) On feeding and supposed buoyancy mechanism in four recent globigerinid foraminifera from the Gulf of Elat, Israel. Rev Esp Micropaleontol 7:325–337
Hemleben C, Spindler M, Breitinger I, Deuser WG (1985) Field and laboratory studies on the ontogeny and ecology of some globorotaliid species from the Sargasso Sea off Bermuda. J Foraminifer Res 15:254–272. https://doi.org/10.2113/gsjfr.15.4.254
Hemleben C, Spindler M, Anderson OR (1989) Modern planktonic foraminifera. Springer, New York
Hofmann DK, Kremer BP (1981) Carbon metabolism and strobilation in *Cassiopea andromedea* (Cnidaria: Scyphozoa): significance of endosymbiotic dinoflagellates. Mar Biol 65:25–33. https://doi.org/10.1007/BF00397064
Hoppe P, Cohen S, Meibom A (2013) NanoSIMS: technical aspects and applications in cosmochemistry and biological geochemistry. Geostand Geoanal Res 37:111–154. https://doi.org/10.1111/j.1751-908X.2013.00239.x
Hottinger L, Dreher D (1974) Differentiation of protoplasm in Nummulitidae (foraminifera) from Elat, Red Sea. Mar Biol 25:41–61
Jørgensen BB, Erez J, Revsbech P, Cohen Y (1985) Symbiotic photosynthesis in a planktonic foraminiferan, *Globigerinoides sacculifer* (Brady), studied with microelectrodes1: symbiotic photosynthesis. Limnol Oceanogr 30:1253–1267. https://doi.org/10.4319/lo.1985.30.6.1253
Kellogg RB, Patton JS (1983) Lipid droplets, medium of energy exchange in the symbiotic anemone *Condylactis gigantea*: a model coral polyp. Mar Biol 75:137–149. https://doi.org/10.1007/BF00405996
Köhler-Rink S, Kühl M (2005) The chemical microenvironment of the symbiotic planktonic foraminifer *Orbulina universa*. Mar Biol Res 1:68–78. https://doi.org/10.1080/17451000510019015
Kopp C, Pernice M, Domart-Coulon I, Djediat C, Spangenberg JE, Alexander DTL, Hignette M, Meziane T, Meibom A (2013) Highly dynamic cellular-level response of symbiotic coral to a sudden increase in environmental nitrogen. mBio 4:e00052-13. https://doi.org/10.1128/mbio.00052-13
Kopp C, Wisztorski M, Revel J, Mehiri M, Dani V, Capron L, Carette D, Fournier I, Massi L, Mouajjah D, Pagnotta S, Priouzeau F, Salzet M, Meibom A, Sabourault C (2015a) MALDI-MS and NanoSIMS imaging techniques to study cnidarian–dinoflagellate symbioses. Zoology 118:125–131. https://doi.org/10.1016/j.zool.2014.06.006
Kopp C, Domart-Coulon I, Escrig S, Humbel BM, Hignette M, Meibom A (2015b) Subcellular investigation of photosynthesis-driven carbon assimilation in the symbiotic reef coral *Pocillopora damicornis*. mBio 6:e02299-14. https://doi.org/10.1128/mbio.02299-14
Krupke A, Mohr W, LaRoche J, Fuchs BM, Amann RI, Kuypers MM (2015) The effect of nutrients on carbon and nitrogen fixation by the UCYN-A–haptophyte symbiosis. ISME J 9:1635–1647. https://doi.org/10.1038/ismej.2014.253
Lee JJ (1983) Perspective on algal endosymbionts in larger foraminifera. Int Rev Cytol 14:49–77
Lee JJ, Zucker W (1969) Algal flagellate symbiosis in the foraminifer *Archaias*. J Protozoology 16:71–81. https://doi.org/10.1111/j.1550-7408.1969.tb02235.x
Lee JJ, Freudenthal HD, Kossoy V, Bé A (1965) Cytological observations on two planktonic Foraminifera, *Globigerina bulloides* d'Orbigny, 1826, and *Globigerinoides ruber* (d'Orbigny, 1839) Cushman, 1927*††‡. J Eukaryot Microbiol 12:531–542
LeKieffre C, Spangenberg JE, Mabilleau G, Escrig S, Meibom A, Geslin E (2017) Surviving anoxia in marine sediments: the metabolic response of ubiquitous benthic foraminifera (*Ammonia tepida*). PLoS ONE 12:e0177604. https://doi.org/10.1371/journal.pone.0177604
LeKieffre C, Bernhard JM, Mabilleau G, Filipsson HL, Meibom A, Geslin E (2018) An overview of cellular ultrastructure in benthic foraminifera: New observations of rotalid species in the context of existing literature. Mar Micropaleontol 138:12–32. https://doi.org/10.1016/j.marmicro.2017.10.005
Leutenegger S (1977) Ultrastructure de foraminifères perforés et imperforés ainsi que de leurs symbiontes. Cah Micropaléontologie 3:1–52
Leutenegger S (1984) Symbiosis in benthic foraminifera; specificity and host adaptations. J Foraminifer Res 14:16–35
Musat N, Stryhanyuk H, Bombach P, Adrian L, Audinot J-N, Richnow HH (2014) The effect of FISH and CARD-FISH on the isotopic composition of ^{13}C- and ^{15}N-labeled *Pseudomonas putida* cells measured by nanoSIMS. Syst Appl Microbiol 37:267–276. https://doi.org/10.1016/j.syapm.2014.02.002
Muscatine L, Karakashian SJ, Karakashian MW (1967) Soluble extracellular products of algae symbiotic with a ciliate, a sponge and a mutant hydra. Comp Biochem Physiol 20:1–12. https://doi.org/10.1016/0010-406X(67)90720-7
Nomaki H, Bernhard JM, Ishida A, Tsuchiya M, Uematsu K, Tame A, Kitahashi T, Takahata N, Sano Y, Toyofuku T (2016) Intracellular isotope localization in *Ammonia* sp. (Foraminifera) of oxygen-depleted environments: results of nitrate and sulfate labeling experiments. Front Microbiol 7:163. https://doi.org/10.3389/fmicb.2016.00163

Nomaki H, LeKieffre C, Escrig S, Meibom A, Yagyu S, Richardson EA, Matsuzaki T, Murayama M, Geslin E, Bernhard JM (2018) Innovative TEM-coupled approaches to study foraminiferal cells. Mar Micropaleontol 138:90–104. https://doi.org/10.1016/j.marmicro.2017.10.002

Nuñez J, Renslow R, Cliff JB, Anderton CR (2018) NanoSIMS for biological applications: current practices and analyses. Biointerphases 13:03B301. https://doi.org/10.1116/1.4993628

Patton JS, Burris JE (1983) Lipid synthesis and extrusion by freshly isolated zooxanthellae (symbiotic algae). Mar Biol 75:131–136. https://doi.org/10.1007/BF00405995

Pernice M, Meibom A, Van Den Heuvel A, Kopp C, Domart-Coulon I, Hoegh-Guldberg O, Dove S (2012) A single-cell view of ammonium assimilation in coral–dinoflagellate symbiosis. ISME J 6:1314–1324

Pernice M, Dunn SR, Tonk L, Dove S, Domart-Coulon I, Hoppe P, Schintlmeister A, Wagner M, Meibom A (2015) A nanoscale secondary ion mass spectrometry study of dinoflagellate functional diversity in reef-building corals. Environ Microbiol 17:3570–3580. https://doi.org/10.1111/1462-2920.12518

Polerecky L, Adam B, Milucka J, Musat N, Vagner T, Kuypers MMM (2012) Look@NanoSIMS—a tool for the analysis of nanoSIMS data in environmental microbiology. Environ Microbiol 14:1009–1023. https://doi.org/10.1111/j.1462-2920.2011.02681.x

Preiss J (1982) Regulation of the biosynthesis and degradation of starch. Annu Rev Plant Physiol 33:431–454

Rhumbler L (1911) Die Foraminiferen (Thalamophoren) der Plankton-Expedition, Teil 1: Die allgemeinen Organisationsverhaltnisse der Foraminiferen

Rink S, Kühl M, Bijma J, Spero HJ (1998) Microsensor studies of photosynthesis and respiration in the symbiotic foraminifer *Orbulina universa*. Mar Biol 131:583–595

Röttger R, Berger WH (1972) Benthic foraminifera: morphology and growth in clone cultures of *Heterostegina depressa*. Mar Biol 15:89–94

RStudio Team (2016) RStudio: Integrated Development for R. RStudio Inc., Boston

Schlichter D, Svoboda A, Kremer BP (1983) Functional autotrophy of *Heteroxenia fuscescens* (Anthozoa: Alcyonaria): carbon assimilation and translocation of photosynthates from symbionts to host. Mar Biol 78:29–38. https://doi.org/10.1007/BF00392968

Schmitz K, Kremer BP (1977) Carbon fixation and analysis of assimilates in a coral-dinoflagellate symbiosis. Mar Biol 42:305–313. https://doi.org/10.1007/BF00402192

Smith AM, Denyer K, Martin C (1997) The synthesis of the starch granule. Annu Rev Plant Biol 48:67–87

Spero HJ (1987) Symbiosis in the planktonic foraminifer, *Orbulina universa*, and the isolation of its symbiotic dinoflagellate, *Gymnodinium béii* sp. nov. J Phycol 23:307–317

Spero HJ (1988) Ultrastructural examination of chamber morphogenesis and biomineralization in the planktonic foraminifer *Orbulina universa*. Mar Biol 99:9–20. https://doi.org/10.1007/BF00644972

Spero HJ, Parker SL (1985) Photosynthesis in the symbiotic planktonic foraminifer *Orbulina universa*, and its potential contribution to oceanic primary productivity. J Foraminifer Res 15:273–281

Taylor DL (1968) *In situ* studies on the cytochemistry and ultrastructure of a symbiotic marine dinoflagellate. J Mar Biol Assoc UK 48:349–366. https://doi.org/10.1017/S0025315400034548

Trench RK (1971) The physiology and biochemistry of Zooxanthellae symbiotic with marine coelenterates. II. Liberation of fixed ^{14}C by Zooxanthellae *in vitro*. Proc R Soc Lond B Biol Sci 177:237–250

Trench RK (1979) The cell biology of plant-animal symbiosis. Annu Rev Plant Physiol 30:485–531

Uhle ME, Spero HJ, Lea DW, Ruddiman WF, Engel MH (1999) The fate of nitrogen in the *Orbulina universa* foraminifera–symbiont system determined by nitrogen isotope analyses of shell-bound organic matter. Limnol Ocean 44:1968–1977

Whitehead LF (2003) Metabolite comparisons and the identity of nutrients translocated from symbiotic algae to an animal host. J Exp Biol 206:3149–3157. https://doi.org/10.1242/jeb.00539

Wilkerson FP, Muller G, Muscatine PL (1983) Temporal patterns of cell division in natural populations of endosymbiotic algae. Limnol Oceanogr 28:1009–1014

Yellowlees D, Rees TAV, Leggat W (2008) Metabolic interactions between algal symbionts and invertebrate hosts. Plant Cell Environ 31:679–694. https://doi.org/10.1111/j.1365-3040.2008.01802.x

Zeeman SC, Kossmann J, Smith AM (2010) Starch: its metabolism, evolution, and biotechnological modification in plants. Annu Rev Plant Biol 61:209–234. https://doi.org/10.1146/annurev-arplant-042809-112301